Gene Expression, Vol. 6, pp. 139-149, 1996
Printed in the USA.

1052-2166/96 $10.00 + .00

Characterization of Mouse Fibronectin Alternative mRNAs Reveals an Unusual Isoform Present Transiently During Liver Development

GRZEGORZ K. GÓRSKI,[1] MICHELE C. AROS, AND PAMELA A. NORTON[2]

Department of Medicine, Jefferson Medical College of Thomas Jefferson University, Philadelphia, PA 19107

Fibronectins are found in many extracellular matrices as well as being abundant plasma proteins. The plasma isoforms of fibronectin, which are synthesized in the adult by liver hepatocytes, differ from those derived from most other cells and tissues due to alternative mRNA splicing. Studies in several vertebrates have indicated that FN alternative splicing is regulated spatially and temporally during development. The mouse represents an attractive organism in which to study the regulation of fibronectin splicing during development, but the patterns of fibronectin alternative splicing were not known for this species. Mouse fibronectin cDNA clones were isolated and sequenced, revealing > 95% identity with rat fibronectin at the amino acid level; all three segments that undergo alternative splicing are well conserved. RNase protection and RT-PCR were used to determine the patterns of alternative splicing that occur in fibroblasts and adult liver, sources of cellular and plasma fibronectins. Only A−B− mRNAs were detected in liver, and three V region variants were observed, corresponding to the protein isoforms V120, V95, and V0. Fibroblasts produced mRNAs that were heterogeneous for A and B splicing, but all RNAs contained V120. These patterns contrast with the embryonic form (B+A+V120). Characterization of fibronectin mRNAs from livers of fetal and newborn mice revealed that a significant level of B+ mRNA was present throughout late gestation, declining at birth. Little A+ mRNA was present, and the adult liver V region pattern was observed at all stages. Thus, fibronectin splicing changes during liver development are noncoordinate. One consequence of this temporal regulation is the transient synthesis of B+ mRNAs, including a novel isoform, B+A−V0.

Fibronectin Alternative mRNA splicing Fetal liver

FIBRONECTINS (FNs) are a family of large adhesive glycoproteins that are found in many basement membranes and extracellular matrices as well as circulating in the blood (22,30). FNs are secreted as dimers, and each monomer is composed principally of three types of repeating units (Types I, II, and III repeats). In all vertebrates examined to date, several forms of FN are produced from a single gene via alternative mRNA splicing at three positions (38,45). Protein domains EIIIA and EIIIB are each encoded by single exons, referred to as A and B; omission of either exon from mature mRNA results in polypeptides lacking the corresponding domain. The V or IIICS region is encoded within a single large exon that is subdivided by use of internal 5′ and/or 3′ splice

Received July 15, 1996; revision accepted September 30, 1996.
[1]Current address: Department of Biochemistry and Molecular Biology, Philadelphia College of Osteopathic Medicine, Philadelphia, PA 19131.
[2]Address correspondence to Pamela A. Norton, Thomas Jefferson University, 1020 Locust St., Room 365, Philadelphia, PA 19107.

sites, resulting in two to five distinct isoforms. The precise locations of the alternative V splice sites vary from one species to another (44), and comparisons between mammals and other vertebrates have suggested that the C-terminal portion of V is relatively divergent compared to the remainder of the molecule (12,13,32).

FNs are essential for proper embryonic development; mice that are homozygous for a disruption of the FN gene die by midgestation with numerous mesenchymal defects (16). However, it is not known whether all FN isoforms are functionally equivalent. RNA analyses in several vertebrates have shown that early embryos make predominantly A+B+V120 FN, whereas in the adult, smaller isoforms generally predominate, with characteristic cell and tissue specificity (3,5,7,13, 15,32,34,37). For instance, plasma FN, which is derived from hepatocytes (54), lacks both A and B segments, and smaller V region isoforms represent a substantial fraction of the total FN protein (8,39,44,50). Thus, alternative FN mRNA splicing events are regulated both temporally and spatially during development, resulting in the production of distinct protein isoforms.

The distinct distributions of alternative FN isoforms readily lead to the hypothesis that the extra segments confer novel activities. Several adhesive activities and other functions have been mapped to the V region (44). The N-terminal 25 amino acids, which can be omitted to yield the V95 isoform, include a binding site for $\alpha 4\beta 1$ integrin (17,21,55). Also, the central portion of V contains sites needed for dimer secretion and for incorporation into blood clots (47,49). The EIIIA segment can promote fibroblast adhesion (56) and activate lipocytes in culture (24). Adhesive activities also have been attributed to EIIIB recently (9), and the segment may influence matrix incorporation (18,27). Thus, although it is likely that each alternative segment possesses specific adhesive activities, understanding of the distinct functions of each individual isoform remains incomplete.

The mouse represents an ideal species in which to evaluate FN functions in vivo using genetic and molecular techniques. However, the pattern of FN alternative splicing has not been determined in the mouse. In the present study, we have isolated and sequenced mouse FN cDNAs surrounding and including all three positions of alternative splicing. We have used these clones and the sequence information to determine that the mouse FN pre-mRNA is subjected to exactly the same alternative splicing events as the rat, with three V region isoforms (48), not five as in humans (20). Moreover, we have established that the changes in FN alternative splicing that occur during liver development are noncoordinate, resulting in the transient production of a previously undescribed mRNA isoform. Thus, the developing liver may be a useful system for studying the regulation of FN alternative splicing as well as the function of the alternative forms.

MATERIALS AND METHODS

Isolation and Sequencing of Mouse Fibronectin cDNA Clones

A λZAPII (Stratagene) library prepared from NIH3T3 mouse embryonic fibroblasts (41) was plated on XL1-Blue and screened using standard procedures (43). The probe was a HindIII-PstI fragment of rat fibronectin cDNA spanning the region from EIIIB to EIIIA [BdP, a slightly truncated version of probe AB (46)]. The gel-purified fragment was labeled with [^{32}P]dCTP by random-primed DNA synthesis using a kit from Boehringer Mannheim following the manufacturer's instructions. Following plaque purification, positive clones were rescued as plasmids by in vivo excision following manufacturer's recommended procedures.

DNA sequencing was performed using a Sequenase kit (US Biochemical Corp.) and either [^{35}S] or [^{33}P]dATP. Sequence was obtained from nested deletions generated using the Erase-A-Base kit (Promega Biotech) or from various subclones, and was determined from both strands. Sequence assembly and analysis employed the Wisconsin Sequence Analysis Package (Genetics Computer Group). The final assembled sequence was based largely on clones mfn2 and mfn3 (Fig. 1). However, the reading frame within mfn2 was disrupted at one position. Two additional base pairs were present at this position in clone mfn1; the insertion of these bases preserved the open reading frame and was presumed to represent the correct sequence. In addition, mfn3 differed at a single position from both mfn2 and mfn4; the latter version was incorporated.

Isolation of RNA From Cells and Tissues

Mouse L-cell fibroblasts were obtained from the laboratory of Dr. M. A. Zern. Mouse livers were obtained from either FVB/N or C3H mice; fetal mice were staged relative to the detection of a copulation plug, which is considered as day E0. Livers were removed, dissected away from other

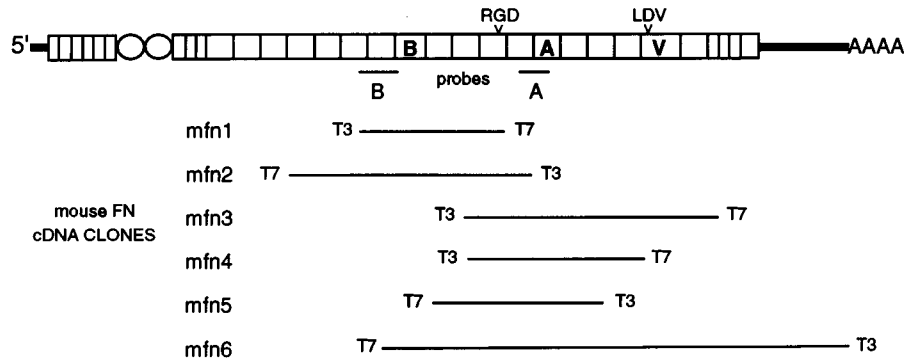

FIG. 1. Structure of cDNA clones and RNase protection probes. At the top is a schematic diagram indicating the modular organization of the FN monomer based on the sequence of other vertebrate FNs (22). Type I repeats are depicted as narrow rectangles, Type II repeats as ovals, Type III repeats as squares, and untranslated regions of the mRNA are shown as thick lines. The alternatively spliced segments are indicated as A, B, and V; major cell adhesion signals are indicated above. The structures of the RNase protection probes are indicated below the schematic (A and B). The portions of the molecule encoded by each cDNA clone are indicated below, and the clones are identified at the left.

tissues, then minced; usually, embryonic livers from two to three animals were pooled at this stage. Some RNA samples were isolated by lysis of cells or minced tissue in guanidinium isothiocyanate followed by ultracentrifugation through a CsCl cushion (10). Alternatively, RNA was isolated by acid guanidinium thiocyanate-phenol-chloroform extraction (11). Commercially prepared Trizol reagent (Gibco/BRL) was added to minced tissue, and RNA was isolated following manufacturer's protocols. The concentration of purified RNA was determined spectrophotometrically and its integrity and concentration were confirmed by agarose gel electrophoresis to visualize 28S and 18S rRNAs.

Preparation of RNA Probes and RNase Protection

Fragments of the cDNAs were subcloned to serve as templates for in vitro transcription. A 480-bp EcoRI-HindIII fragment was isolated from mfn1 and subcloned into pBS− (Stratagene) cut with the same enzymes to create a template for an EIIIB probe. A 250-bp StyI-BstEII fragment was isolated from mfn5, treated with the Klenow fragment of DNA polymeraseI, and subcloned into the EcoRV site of pSKII− (Stratagene) to create a template for an EIIIA probe. Following linearization with EcoRI (B template) or HindIII (A template), in vitro transcription was performed in the presence of [^{32}P]UTP (New England Nuclear) with T3 RNA polymerase using a kit (Stratagene). RNA probes were isolated by denaturing polyacrylamide gel electrophoresis. Probes were eluted from the gel slices in 0.3 M sodium acetate, 0.5% SDS. The recovered probes were resuspended in 100 μl of water.

RNase protection was performed using modifications of published procedures (19). Typically, 1–2 μl of probe ($> 10^5$ cpm/μl probe) was mixed with 5 μg of total RNA (in 1–5 μl H_2O) and 40–45 μl 6 M guanidinium isothiocyanate. Samples were heated to 65°C for 15 min, and incubated overnight at 45°C. Following the addition of 500 μl of 0.75× SSC containing RNaseA (10 μg) and RNase T1 (50 units), the samples were incubated at 45°C for 30 min. RNase-resistant fragments were precipitated by the addition of 1.0 ml ethanol containing 2% diethylpyrocarbonate and 5 μg carrier yeast tRNA. The RNA was collected by microcentrifugation and resuspended in 90% formamide containing 0.1% each bromphenol blue and xylene cyanol and 1 mM EDTA. Samples were heated to 90°C then applied to a 6% denaturing gel. Dried gels were exposed to a PhosphorImage screen (Molecular Dynamics), and the resulting images cropped and contrast adjusted using NIH Image (W. Rasband, NIH).

Reverse Transcription and Polymerase Chain Reaction

Approximately 1 μg of each RNA was incubated with 1.0 μl random hexamers (50 μM) in a total of 10 μl and heated to 70°C for 5–10 min, then chilled on ice. Samples were adjusted to 50 mM Tris-HCl, pH 8.3, 75 mM KCl, 3.0 mM $MgCl_2$, 1.0 mM DTT, 1.0 μl RNAse block (Stratagene), 500 μM dNTPs, and 1.0 μl Superscript re-

verse transcriptase (LifeTechnologies, Inc.); reactions were incubated at 37°C for at least 1 h. The cDNAs were used immediately in PCR reactions or were stored at −20°C.

PCR was performed using either Taq DNA polymerase or Elongase enzyme mixture; no differences were observed in the band patterns produced by the two enzyme preparations. For the former, PCR conditions were 50 mM KCl, 10 mM Tris-HCl, pH 8.3, 1.5 mM $MgCl_2$, 0.2 mM each dATP, dCTP, dGTP, and dTTP, 25–50 pmol each primer, 2.5 units Taq DNA polymerase (Stratagene or Perkin-Elmer/Cetus), and 1 μl cDNA in a total of 100 μl. PCR was performed for 35 cycles: 94°C, 1 min, 50°C, 1 min, and 72°C, 1 min, with a final extension of 7 min at 72°C. Elongase reactions (LifeTechnologies, Inc.) were prepared with manufacturers' supplied reagents in a 50 μl total volume. Amplifications were for 30–35 cycles, with little variation observed with increased cycle number (not shown). A list of primers used is shown in Table 1. After electrophoresis through agarose or polyacrylamide, products were visualized by staining with ethidium bromide and photographed. Photos were scanned, and the images were reversed, contrast adjusted, and cropped in NIH Image.

RESULTS

Isolation and Sequencing of Mouse Fibronectin cDNA Clones

A cDNA library prepared from mouse NIH3T3 embryonic fibroblasts was screened using a fragment of rat cDNA. Screening of ca. 4×10^4 plaques yielded six positive clones; the structures of these are diagrammed in Fig. 1. These clones, termed mfn1–6, span all three regions known to undergo alternative splicing, indicated in the figure as A, B, and V. Two of the clones, mfn2 and mfn3, were sequenced in entirety, and portions of the other clones were also sequenced (see Materials and Methods section). A subclone of mfn6 was sequenced to bridge a short gap between mfn3 and a previously sequenced segment of the 3′ end of mouse FN (4). The newly determined composite sequence (4435 base pairs) is 94.5% identical to rat FN (data not shown; accession number X93167). The predicted amino acid sequence is shown in Fig. 2; the mouse and rat sequences are 96% identical, with most changes being conservative substitutions. Specific features of the predicted protein sequence are considered in more detail in the Discussion section.

Determination of the Mouse FN Splicing Pattern

Fragments of mfn1 and mfn5 were subcloned to serve as RNase protection probes for exons EIIIB and EIIIA, respectively, as indicated in Fig. 1. Based on studies of other species (13,26,32, 36,46), we anticipated that adult liver FN mRNA would be B−A−, whereas fibroblasts would contain some B+ and/or A+ mRNAs. RNase protection analyses of total RNA derived from fibroblasts using the B probe produced bands of 480 and 453 bp, representing B+ and B− forms (Fig. 3A, lane 3). In contrast, only the B− form was detected in liver RNA (lane 4). When the A probe was hybridized to fibroblast RNA, bands of 250 and 148 bp were detected (Fig. 3B, lane 3), representing A+ and A− forms, but only A− mRNA was detected in liver (lane 4). Thus, splicing of these two alternative segments is the same in the mouse as in other species.

In the rat, three V region isoforms (V120, V95, and V0) are present in the adult liver, but predominantly the full-length V120 is detected in fibroblasts (44). This pattern is distinct from the five isoforms observed in human liver (20), and thus it was necessary to verify the mouse V splicing pattern experimentally. RT-PCR analysis of adult mouse liver RNA was performed using primers

TABLE 1
PRIMERS USED FOR PCR EXPERIMENTS

Primer	Sequence (5′ → 3′)	Usage
VF	GCTACATTATCAAGTATGAG	forward primer 5′ of V
VR	AATGATGTACTCAGAACTCT	reverse primer 3′ of V
AF	GAAATGACCATTGAAGGTTTG	forward primer 5′ of A
AR	TTCTTTCATTGGTCCTGTCTT	reverse primer 3′ of A
BF	CATGCTGATCAGAGTTCCTG	forward primer 5′ of B
BR	GGTGAGTAGCGCACCAAGAG	reverse primer 3′ of B
IBF	TACCGAATCACAGTAGTTGC	forward primer within B

```
                          W         Y                                L     Y
III4 DNVPPPTDLQFVELTDVKVTIMWTPPDSV VSGYRVEVLPVSLPGEH GQRLPVNRNTFAEITGLSPGVTYLFKVFAVHQGRESNPLTAQQTT
III5  KLDAPTNLQFVNETDRTVLVTWTPPRAR IAGYRLTAGLTRGGQPKQ  YNVGPLASKYPLRNLQPGSEYTATLVAVKGNQQSPKATGVFTTL
III6  QPLRSIPPYNTEVTETTIVITWTPAPR   IGFKLGVRPSQGGEAPRE   VTSDSGSIVVSGLTPGVEYTYTIQVLRDGQERDAPIVNRVVTP
III7  LSPPTNLHLEANPDTGVLTVSWERSTTPDITGYRITTTPTNGQQGTSLEEVVHADQSSCTFENLNPGLEYNVSVYTVKDDKESAPISDTVVP
IIIB   EVPQLTDLSFDITDSSIGLRWTPLNSSTIIGYRITVVAAGEGIP IFEDFVDSSVGYYTVTGLEPGIDYDISVITLINGGESAPTTLTQQT
III8  AVPPPTDLRFTNIGPDTMRVTWAPPPSIELTNLLVRYSPVKNEED VAELSISPSDNAVVLTNLLPGTEYLVSVSSVYEQHESIPLRGRQKT
III9  GLDSPTGFDSSDITANSFTVHWVAPRAP ITGYIIRHHAEHSVGR PRQDRVPPSRNSITLTNLNPGTEYVVSIIAVNGREESPPLIGQQAT
III10 VSDIPRDLEVIASTPTSLLISWEPPAVSV RYYRITYGETGGNSP VQEFTVPGSKSTATINNIKPGADYTITLYAVTGRGDSPASSKPVSINYKT
III11 EIDKPSQMQVTDVQDNSISVRWLPSTSP VTGYRVTTTPKNGLGP SKTKTASPDQTEMTIEGLQPTVEYVVSVYAQNRNGESQPLVQTAVT
IIIA  NIDRPKGLAFTDVDVDSIKIAWESPQGQ VSRYRVTYSSPEDGIRE LFPAPDGEDDTAELQGLRPGSEYTVSVVALHDDMESQPLIGIQST
III12 AIPAPTNLKLSQVTPTSFTAQWIAPSVQ LTGYRVRVNPKEKTGPM KEINLSPDSSSVIVSGLMVATKYEVSVYALKDTLTSRPAQGVITTLE
III13 NVSPPRRARVTDATETTITISWRTKTET ITGFQVDAIPANGQTPV  QRSISPDVRSYTITGLQPGTDYKIHLYTLNDNARSSPVIIDAST
III14 AIDAPSNLRFLTTTPNSLLVSWQAPRAR ITGYIIKYEKPGSPPREVV PRPRPGVTEATITGLEPGTEYTIYVIALKNNQKSEPLIGRKKT
V25                              DELPQLVTLPHPNLHGPEILDVPST
V95    VQKTPFITNPGYDTENGIQLPGTTHQQPSVGQQMIFEEHGFRRTTPPTAATPVRLRPRPYLPNVDEEVQIGHVPRGDVDYHLYPHVPGLNPNAST
III15            GQEALSQTTISWTPFQESSEYIISCQPVGTDEEPLQFQVPGTSTSATLTGLTRGVTYNIIVEALQNQRRHKVREEVVTVGNA
I10         VSEGLNQPTDDSCFDPYTVSHYAIGEEWERLSDAGFKLTCQCLGFGSGHFRCDSS
I11                    KWCHDN  GVNYKIGEKWDRQGENGQRMSCTCLGNGKGEF
```

FIG. 2. Deduced partial mouse FN protein sequence. The composite sequence was derived from sequencing mfn3 in entirety, most of mfn2, and small portions of the other clones. The sequence is presented to emphasize the repeating structure of the protein; conserved residues characteristic of FN Type III repeat units are indicated above the aligned sequences. Key features are underlined and described in the text.

that flank the V region (Table 1); this analysis revealed three bands of 607, 532, and 247, as predicted for V120, V95, and V0 isoforms (Fig. 3C, lanes 2 and 3). Only the band corresponding to V120 was produced when fibroblast RNA was used as template (lane 1). The precise position of the alternative splice sites used in mouse was determined by subcloning and sequencing of the PCR products. This analysis confirmed that the positions of the alternative 3′ splice sites are identical in mouse and rat, subdividing the region into V25 and V95 segments (Fig. 2). Densitometric analyses established that over 80% of the FNs present in both adult liver samples were V0, slightly higher than the value of 75% previously reported in the rat (26). Thus, FN alternative splicing in the

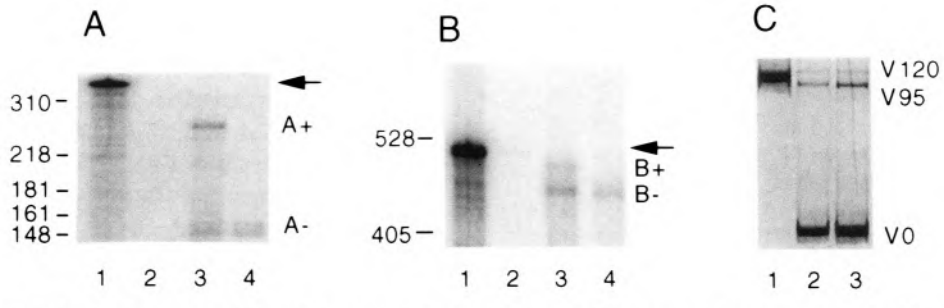

FIG. 3. Establishment of FN splicing pattern in the mouse. (A) RNase protection analysis of fibroblast and liver RNAs with a probe specific for the A exon. Samples were applied to a denaturing 6% polyacrylamide gel; lane 1, probe alone (arrow); lane 2, yeast tRNA control; lane 3, fibroblast RNA; lane 4, liver RNA. Fibroblasts contain both forms; liver contains only A− mRNAs. (B) RNase protection analysis of fibroblast and liver RNA with a probe specific for the B exon. Samples were analyzed and lanes loaded as in (A); arrow indicates position of intact probe. Fibroblasts contain both forms; liver contains only B− mRNAs. (C) RT-PCR analysis of V region splicing. Primers that flank the V region were used in PCR amplification of cDNA prepared from fibroblast (lane 1) or liver RNAs (lanes 2 and 3, independent preparations); after 35 cycles of amplification, samples were analyzed on a 6% nondenaturing polyacrylamide gel. Products of 607, 532, and 247 bp were observed for liver, but only the largest was detected in fibroblasts. The precise boundaries of the smaller forms were confirmed by cloning and sequencing of the amplified products; the resulting protein subdomains are indicated in Fig. 2.

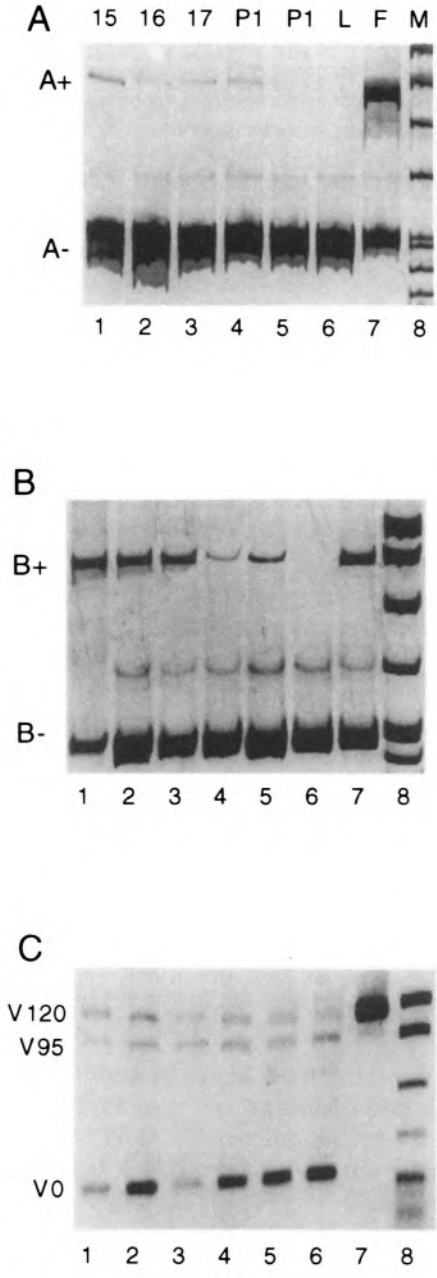

FIG. 4. FN isoforms present during liver development. RT-PCR analysis of liver RNAs isolated from E15 (lanes 1), E16 (lanes 2), E17 (lanes 3), postnatal day 1 (lanes 4 and 5), and adult (lane 6) mice and from fibroblasts (lane 7). Lanes M, MspI cut pBR322; from top bands are 622, 527, 404, 309, 242/238, 217, 201. Note that not all bands are visible in every panel, but the uppermost band always corresponds to the 622-bp fragment. The light bands present in (A) and (B) between the labeled products are PCR artifacts of unknown origin that are not always evident. Also, the E16 sample seems to consistently give a stronger signal than the other embryonic samples, but changes in cycle number did not change the patterns observed (not shown). (A) Amplification of A+ and A− species (515 and 245 bp); samples were analyzed after 35 cycles on a 6% nondenaturing polyacrylamide gel. (B) Amplification of B+ and B− species (505 and 232); samples were analyzed after 35 cycles on a 6% nondenaturing polyacrylamide gel. (C) Amplification of V120, V95, and V0 species (607, 532, and 247 bp); samples were analyzed after 30 cycles on a 2% agarose gel.

mouse is qualitatively and quantitatively similar to that of the rat.

Changes in FN Splicing Pattern During Liver Development

In early embryos of several vertebrates, FN mRNAs containing all three alternative regions predominate, with tissue-specific loss of segments observed during development (13,15,32,35,37). These and other studies showed that in the adult liver, EIIIA and EIIIB are completely excluded and > 50% of mRNAs lack all or part of the V region; the experiments in Fig. 3 extend these findings to include the mouse. We have also observed that early mouse embryos contain predominantly B+A+ FN mRNAs (unpublished data). Thus, changes in alternative splicing must occur at all three positions during liver development.

Total RNA was isolated from livers of late fetal and newborn mice and analyzed by RT-PCR to investigate the temporal sequence of splicing changes (gestation is ca. 19 days). The RT-PCR data are shown in Fig. 4; these were quantitated by scanning densitometry (Table 2), and the results are concordant with RNAse protection analyses performed on some of the same samples (Fig. 3 and data not shown). At all embryonic and postnatal stages examined, the V region splicing pattern resembled that of the adult (Fig. 4C, compare lanes 1–5 with lane 6), although there was some variablility in the precise ratios of the isoforms (Table 2). Similarly, most of the FN mRNA in fetal and newborn liver was A− (Fig. 4A, lanes 1–5). In contrast, a significant fraction of FN mRNA present at all embryonic days tested was B+ (Fig. 4B, lanes 1–3, Table 2), and a small amount was detected in the livers of newborns (Fig. 4B, lanes 4 and 5). Thus, splicing changes begin early during tissue development, and the shift from B+ to B− is not temporally coordinated with changes in A and V.

B+V0 mRNAs have not been detected previously in vivo. The significant quantities of B+ mRNAs present at E15–17 suggested that some fraction of these also may be V0. This possibility was tested by performing PCR using the reverse V region primer and a forward primer internal to B. Two products of ca. 2.5 and 2.1 kbp were amplified from cDNA prepared from E17 liver mRNA (Fig. 5). These fit well with the predicted sizes of 2512 for V120, 2437 for V95, and 2152 for V0; presumably, the V120 and V95 forms were not resolved. The structure of these amplified products was confirmed by digestion of the PCR prod-

TABLE 2
QUANTITATION OF SPLICING CHANGES DURING LIVER DEVELOPMENT

Stage	%A− FN	%B− FN	%V95 FN	%V0 FN
E15	95	54	16	58
E16	99	72	9	77
E17	98	72	32	47
P1	99	92	15	75
Adult	100	100	12	85
Fibroblasts	50	73	<2	<2

ucts with BamHI. A large fragment was liberated (not shown), along with three smaller fragments representing the three V region variants (Fig. 5). The relative ratios of the three isoforms observed in this experiment agreed with their relative abundance in total FN mRNA (Fig. 4C, Table 2), suggesting that B and V are independently regulated. Thus, a novel FN mRNA isoform, B+A−V0 is present in fetal liver, representing more than 10% of the total FN mRNA.

DISCUSSION

Features of the Mouse FN Sequence

Sequencing of cDNA clones representing nearly 4.5 kbp of mouse FN mRNA reveals > 90% identity to other mammalian FNs within the coding region, in agreement with an earlier report of the 3′ ca. 1.0 kbp of the mRNA (4), and a recent report of a smaller fragment that lies slightly 5′ to our sequence (53). Thus, it is not surprising to find that several adhesion sites characterized in human or rat FNs are conserved in the mouse (Fig. 2). The critical GRGDSP motif is recognized by several integrin receptor heterodimers, including $\alpha 5\beta 1$ (42). A sequence required for $\alpha IIb\beta 3$ interaction with FN, DRVPHSRNSIT, is largely conserved (P substituted for H in the mouse) (6). This sequence corresponds to one of a pair of sites that synergize with the RGD motif for $\alpha 5\beta 1$ adhesion to FN (1). A binding site for $\alpha 4\beta 1$ integrin, with the core motif IDAPS is present in the C-terminal heparin domain (31). Other adhesive sites for heparin and other proteoglycans in repeats III13 and 14 are also conserved (2,14,23,28). Thus, mouse FN is most likely indistinguishable functionally from the previously characterized human and rat proteins.

Nonetheless, careful comparison between mouse, rat, and human FNs reveals that certain regions display greater than average divergence. The plot of similarity of mouse, rat, and human FNs shown in Fig. 6 suggests that III5, as well as the C-terminal portion of EIIIA along with a portion of neighboring III12, is less well conserved than other regions. The V segment appeared to be the most divergent region of FN when comparisons were made between mammalian FNs and those of nonmammalian vertebrates (13,32), but V is not especially divergent when the comparison is restricted to mammalian FNs (Fig. 6). This conservation may reflect the acquisition of functions specific to mammals. The C-terminal portion of V is very poorly conserved in nonmammalian vertebrates (Fig. 7). However, manipulation of the alignment reveals a moderately conserved motif within the CS5 peptide, represented as RGD. This motif or a related sequence (HGD or RED) is present in all species except chicken; interestingly, the chicken is the only species in which this motif is present in all isoforms (32).

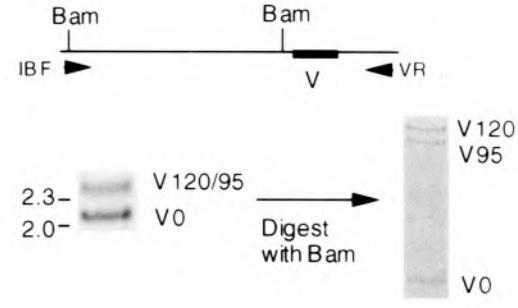

FIG. 5. Detection of a B+A−V0 FN mRNA isoform. At the top is a diagram of the experimental strategy to determine the V composition of mRNAs that contain B. Below left, RT-PCR analysis of E17 liver RNA using IBF and VR primers; sample was subjected to 35 cycles of amplification and analyzed on a 1% agarose gel. Only two bands were observed, corresponding to V120/V95 (bands of 2512 and 2437 bp did not resolve) and V0 (2152 bp); thus, there was no evidence for either additional variants or incompletely processed RNAs. Another aliquot of this sample was cut with BamHI and the products resolved on a 6% polyacrylamide gel (right). A single large fragment was observed (> 1.0 kbp, not shown) as well as three smaller fragments correponding to the expected sizes of 550, 475, and 190 bp for the V120, V95, and V0 RNA isoforms.

Characterization of Mouse FN Alternative Splicing

The similarity of the rat and mouse splicing patterns was expected, but it was necessary to confirm the pattern of splicing in the mouse experimentally, especially for the V region, where considerable interspecies heterogeneity occurs (44). The data presented demonstrate that mouse and rat FN mRNAs undergo identical alternative splicing events. Specifically, the pattern of FN splicing in mouse liver is identical to that of the rat (26,37,46,48). However, the data presented here extend previous observations by examination of several stages during mouse liver development. This analysis revealed that splicing changes at different positions are not coordinated during liver development. Splicing at the V region in E15–16 liver was indistinguishable from that of the adult liver, and A− mRNAs were predominant throughout the late fetal period. In contrast, significant levels of B+ RNAs were present during the late fetal period, declining perinatally. This staggered temporal sequence results in the transient production of a novel isoform, B+A−V0.

Other workers have characterized FN mRNAs in the liver at single embyonic stages, and all reports agree that fetal liver has a higher proportion of B+A+ FN than adult. Pagani et al. (37) found that E17 fetal rat liver contained significant levels of B+, but detected higher levels of the A+ and V120 forms than shown in Fig. 4. Oyama et al. (34) analyzed FN mRNAs isolated from midgestation human fetal livers, and observed similar levels of A and B (ca. 25%), but fairly low levels of forms equivalent to V95 and V0. Our embryonic samples represent pools isolated from two or more livers, to reduce individual variation. The differences in our observations could represent interspecies differences, or could be due to specimens of nonequivalent gestational age.

Identification of a Novel FN Isoform

The data in Fig. 5 demonstrate the existence of a novel FN isoform, B+A−V0 in the late fetal liver, suggesting that the corresponding protein isoforms fulfill a specific but transient function at this time. Evidence points to the liver (33), and specifically to hepatocytes (54) as the source of plasma FN in adult animals. As the liver is a major hematopoietic organ in the fetal mouse (29), it is attractive to speculate that this role requires the presence of novel matrix components. However, the loss of B+ mRNAs perinatally also coincides with increased hepatocyte polarization, and it has

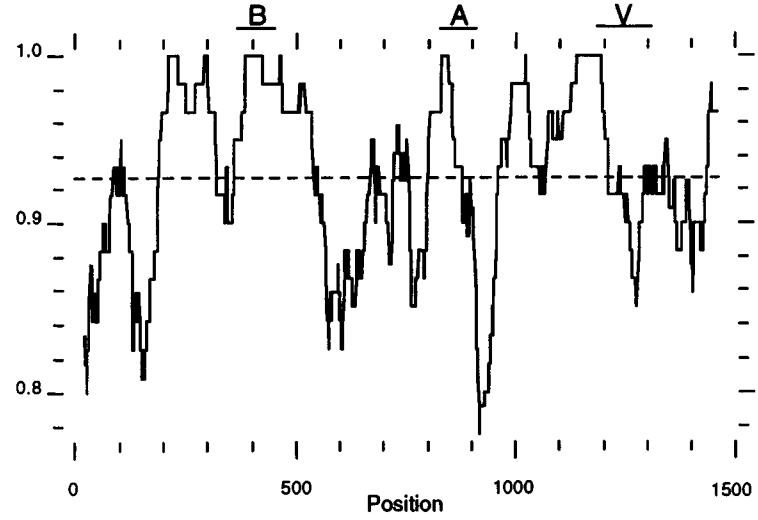

FIG. 6. Similarity plot of mouse, human, and rat fibronectins. Amino acid sequences translated from human (Genbank K00799, with M18177, the human EIIIB sequence, added to it) and rat (X15906) FN sequences were aligned with the partial mouse sequence shown in Fig. 2. These aligned sequences were then analyzed for the level of identity (scale at left) by the Plotsimilarity program, with a sliding window of 40. The average level of identity is indicated by the dotted horizontal line; identities were assigned a score of 1.0; nonidentities, 0. Regions of the protein that are subjected to exclusion by alternative splicing are indicated by the labeled bars at the top.

FIG. 7. V region sequence comparison. The sequences of the V regions of seven vertebrate FNs are shown. P, *Pleurodeles waltii* (12), X, *Xenopus laevis* (13), C, *Gallus domesticus* (32); H, *Homo sapiens* (25); B, *Bos tarsus* (51); R, *Rattus norvegicus* (48); M, *Mus musculus* (this study). Vertical lines indicate identities, and asterisks highlight residues shared by all species. The LDV cell adhesion site is indicated by underlining. A consensus for a second adhesion signal is shown at the bottom (RGD; see text).

been suggested that cell-FN interactions could be important prior to the establishment of cell-cell adhesions (52). Thus, the B segment may play an important role in the cell-matrix interactions that precede the formation of cell-cell interactions characteristic of mature liver.

Although the present study was restricted to characterizing variant FNs at the mRNA level, the data predict that hepatocytes may produce B+ FN protein. It remains to be determined whether FNs containing B+ and A+ are secreted into plasma or are retained in the liver. A very low level of B+ FN was detected in normal adult plasma (40), but it is not known whether this material originated in the liver or was derived from other cells such as platelets and endothelial cells, both of which produce B+ FNs. Thus, further studies are needed to establish whether B+ isoforms are present stoichiometrically in plasma, as well as to identify the cells that are the source of B+ FNs. These studies may also provide insight into the functional significance of these isoforms.

ACKNOWLEDGEMENTS

We thank R. Perkinson and R. McInnis for technical assistance. We are grateful to Drs. V. Bennett, J. Kuncio, and B. Kuo for thoughtful comments on the manuscript. Portions of this work were supported by a grant (GM-46402) from the National Institutes of Health and by funds from Jefferson Medical College (to P.A.N.).

REFERENCES

1. Aota, S.-I.; Nagai, T.; Yamada, K. M. Characterization of regions of fibronectin besides the arginine-glycine-aspartic acid sequence required for adhesive function of the cell-binding domain using site-directed mutagenesis. J. Biol. Chem. 266: 15938–15943; 1991.
2. Barkalow, F. J. B.; Schwarzbauer, J. E. Localization of the major heparin-binding site in fibronectin. J. Biol. Chem. 266:7812–7818; 1991.
3. Bennett, V. D.; Pallante, K. M.; Adams, S. L. The splicing pattern of fibronectin mRNA changes during chondrogenesis resulting in an unusual form of the mRNA in cartilage. J. Biol. Chem. 266:5918–5924; 1991.

4. Blatti, S. P.; Foster, D. N.; Ranganathan, G.; Moses, H. L.; Getz, M. J. Induction of fibronectin gene transcription and mRNA is a primary response to growth-factor stimulation of AKR-2B cells. Proc. Natl. Acad. Sci. USA 85:1119–1123; 1988.
5. Borsi, L.; Balza, E.; Allemanni, G.; Zardi, L. Differential expression of the fibronectin isoform containing the ED-B oncofetal domain in normal fibroblast cell lines originating from different tissues. Exp. Cell Res. 199:98–105; 1992.
6. Bowditch, R. D.; Hariharan, M.; Tominna, E. F.; Smith, J. W.; Yamada, K. M.; Getzoff, E. D.; Ginsberg, M. H. Identification of a novel integrin binding site in fibronectin: Differential utilization by $\beta 3$ integrins. J. Biol. Chem. 269:10856–10863; 1994.
7. Carnemolla, B.; Balza, E.; Siri, A.; Zardi, L.; Nicotra, M. R.; Bigotti, A.; Natali, P. G. A tumor-associated fibronectin isoform generated by alternative splicing of messenger RNA precursors. J. Cell Biol. 108:1139–1148; 1989.
8. Castellani, P.; Siri, A.; Rosellini, C.; Infusini, E.; Borsi, L.; Zardi, L. Transformed human cells release different fibronectin variants than do normal cells. J. Cell Biol. 103:1671–1677; 1986.
9. Chen, W.; Culp, L. A. Adhesion mediated by fibronectin's alternatively spliced EDb (EIIIB) and its neighboring type III repeats. Exp. Cell Res. 223:9–19; 1996.
10. Chirgwin, J. M.; Przybyla, A. E.; MacDonald, R. J.; Rutter, W. J. Isolation of biologically active ribonucleic acid from sources enriched in ribonuclease. Biochemistry 18:5194–5199; 1979.
11. Chomczynski, P.; Sacchi, N. Single step method of RNA isolation by acid guanidinium thiocyanate-phenol-chloroform extraction. Anal. Biochem. 162: 156–159; 1987.
12. Clavilier, L.; Riou, J.-F.; Shi, D. L.; DeSimone, D. W.; Boucaut, J.-C. Amphibian Pleurodeles waltl fibronectin: cDNA cloning and developmental expression of spliced variants. Cell Adhes. Commun. 1:83–91; 1993.
13. DeSimone, D. W.; Norton, P. A.; Hynes, R. O. Identification and characterization of alternatively spliced fibronectin mRNAs expressed in early *Xenopus* embryos. Dev. Biol. 149:357–369; 1992.
14. Drake, S. L.; Varnum, J.; Mayo, K. H.; Letourneau, P. C.; Furcht, L. T.; McCarthy, J. B. Structural features of fibronectin synthetic peptide FN-C/HII, responsible for cell adhesion, neurite extension, and heparan sulfate binding. J. Biol. Chem. 268:15859–15867; 1993.
15. French-Constant, C.; Hynes, R. O. Alternative splicing of fibronectin is temporally and spatially regulated in the chicken embryo. Development 106: 375–388; 1989.
16. George, E. L.; Georges-Labouesse, E. N.; Patel-King, R. S.; Rayburn, H.; Hynes, R. O. Defects in mesoderm, neural tube and vascular development in mouse embryos lacking fibronectin. Development 119:1079–1091; 1993.
17. Guan, J.-L.; Hynes, R. O. Lymphoid cells recognize an alternatively spliced segment of fibronectin via the integrin receptor $\alpha 4\beta 1$. Cell 60:53–61; 1990.
18. Guan, J.-L.; Trevithick, J. E.; Hynes, R. O. Retroviral expression of alternatively spliced forms of rat fibronectin. J. Cell Biol. 110:833–847; 1990.
19. Haines, D. S.; Gillespie, D. H. RNA abundance measured by a lysate RNase protection assay. BioTech 12:736–741; 1992.
20. Hershberger, R. P.; Culp, L. A. Cell-type-specific expression of alternatively spliced human fibronectin IIICS mRNAs. Mol. Cell. Biol. 10:662–671; 1990.
21. Humphries, M. J.; Komoriya, A.; Akiyama, S. K.; Olden, K.; Yamada, K. M. Identification of two distinct regions of the type III connecting segment of human plasma fibronectin that promote cell type-specific adhesion. J. Biol. Chem. 262:6886–6892; 1987.
22. Hynes, R. O. Fibronectins. New York: Springer-Verlag; 1990.
23. Jalkanen, S.; Jalkanen, M. Lymphocyte CD44 binds the COOH-terminal heparin-binding domain of fibronectin. J. Cell Biol. 116:817–825; 1992.
24. Jarnagin, W. R.; Rockey, D. C.; Koteliansky, V. E.; Wang, S.-S.; Bissell, D. M. Expression of variant fibronectins in wound healing: Cellular source and biological activity of the EIIIA segment in rat hepatic fibrosis. J. Cell Biol. 127:2037–2048; 1994.
25. Kornblihtt, A. R.; Umezawa, K.; Vibe-Pedersen, K.; Baralle, F. E. Primary structure of human fibronectin: Differential splicing may generate at least 10 polypeptides from a single gene. EMBO J. 4:1755–1759; 1985.
26. Magnuson, V. L.; Young, M.; Schattenberg, D. G.; Mancini, M. A.; Chen, D.; Steffensen, B.; Klebe, R. J. The alternative splicing of fibronectin pre-mRNA is altered during aging and in response to growth factors. J. Biol. Chem. 266:14654–14662; 1991.
27. Mardon, H. J.; Grant, R. P.; Grant, K. E.; Harris, H. Fibronectin splice variants are differentially incorporated into the extracellular matrix of tumorigenic and non-tumorigenic hybrids between normal fibroblasts and sarcoma cells. J. Cell Sci. 104:783–792; 1993.
28. McCarthy, J. B.; Skubitz, A. P. N.; Zhao, Q.; Yi, X.-Y.; Mickelson, D. J.; Klein, D. J.; Furcht, L. T. RGD-independent cell adhesion to the carboxy-terminal heparin-binding fragment of fibronectin involves heparin-dependent and -independent activities. J. Cell Biol. 110:777–787; 1990.
29. Medlock, E. S.; Haar, J. L. The liver hemopoietic environment: I. Developing hepatocytes and their role in fetal hemopoiesis. Anat. Rec. 207:32–41; 1983.
30. Mosher, D. F., ed. Fibronectin. London: Academic Press; 1989.
31. Mould, A. P.; Humphries, M. J. Identification of a novel recognition sequence for the integrin $\alpha 4\beta 1$ in

the COOH-terminal heparin-binding domain of fibronectin. EMBO J. 10:4089–4095; 1991.
32. Norton, P. A.; Hynes, R. O. Alternative splicing of chicken fibronectin in embryos and in normal and transformed cells. Mol. Cell. Biol. 7:4297–4307; 1987.
33. Owens, M. R.; Cimino, C. D. Synthesis of fibronectin by the isolated perfused rat liver. Blood 59:1305–1309; 1982.
34. Oyama, F.; Hirohashi, S.; Sakamoto, M.; Titani, K.; Sekiguchi, K. Coordinate oncodevelopmental modulation of alternative splicing of fibronectin pre-messenger RNA at ED-A, ED-B, and CS1 regions in human liver tumors. Cancer Res. 53:2005–2011; 1993.
35. Oyama, F.; Murata, Y.; Suganuma, N.; Kimura, T.; Titani, K.; Sekiguchi, K. Patterns of alternative splicing of fibronectin pre-mRNA in human adult and fetal tissues. Biochemistry 28:1428–1434; 1989.
36. Pagani, F.; Zagato, L.; Coviello, D.; Vergani, C. Alternative splicing of fibronectin pre-mRNA during aging. Ann. NY Acad. Sci. 663:477–8; 1992.
37. Pagani, F.; Zagato, L.; Vergani, C.; Casari, G.; Sidoli, A.; Baralle, F. E. Tissue specific splicing pattern of fibronectin messenger RNA during development and aging in rat. J. Cell Biol. 113:1223–1229; 1991.
38. Paolella, G.; Barone, M. V.; Baralle, F. E. Fibronectin. In: Zern, M. A.; Reid, L. M., eds. Extracellular matrix. Chemistry, biology and pathobiology with emphasis on the liver. New York: Marcel Dekker; 1993:3–24.
39. Paul, J. I.; Schwarzbauer, J. E.; Tamkun, J. W.; Hynes, R. O. Cell-type-specific fibronectin subunits generated by alternative splicing. J. Biol. Chem. 261:12258–12265; 1986.
40. Peters, J. H.; Trevithick, J. E.; Johnson, P.; Hynes, R. O. Expression of the alternatively spliced EIIIB segment of fibronectin. Cell Adhes. Commun. 3: 67–89; 1995.
41. Rees, D. J.; Ades, S. E.; Singer, S. J.; Hynes, R. O. Sequence and domain structure of talin. Nature 347: 685–689; 1990.
42. Ruoslahti, E.; Pierschbacher, M. D. New perspectives in cell adhesion: RGD and integrins. Science 238:291–297; 1987.
43. Sambrook, J.; Fritsch, E. F.; Maniatis, T. Molecular cloning: A laboratory manual, 2nd ed. Cold Spring Harbor, NY: Cold Spring Harbor Laboratory Press; 1989.
44. Schwarzbauer, J. E. Alternative splicing of fibronectin: Three variants, three functions. Bioessays 13:527–533; 1991.
45. Schwarzbauer, J. E. Fibronectin: From gene to protein. Curr. Opin. Cell Biol. 3:786–791; 1991.
46. Schwarzbauer, J. E.; Patel, R. S.; Fonda, D.; Hynes, R. O. Multiple sites of alternative splicing of the rat fibronectin gene transcript. EMBO J. 6: 2573–2580; 1987.
47. Schwarzbauer, J. E.; Spencer, C. S.; Wilson, C. L. Selective secretion of alternatively spliced fibronectin variants. J. Cell Biol. 109:3445–3453; 1989.
48. Schwarzbauer, J. E.; Tamkun, J. W.; Lemischka, I. R.; Hynes, R. O. Three different fibronectin mRNAs arise by alternative splicing within the coding region. Cell 35:421–431; 1983.
49. Schwarzbauer, J. E.; Wilson, C. L. The alternatively spliced V region contributes to the differential incorporation of plasma and cellular fibronectins into fibrin clots. J. Cell Biol. 119:923–933; 1992.
50. Sekiguchi, K.; Titani, K. Probing molecular polymorphisms of fibronectins with antibodies directed to the alternatively spliced peptide segments. Biochemistry 28:3293–3298; 1989.
51. Skorstengaard, K.; Jensen, M. S.; Petersen, T. E.; Magnusson, S. Complete primary structure of bovine plasma fibronectin. Eur. J. Biochem. 161:441–453; 1986.
52. Stamatoglou, S. C.; Enrich, C.; Manson, M. M.; Hughes, R. C. Temporal changes in the expression and distribution of adhesion molecules during liver development and regeneration. J. Cell Biol. 116: 1507–1515; 1992.
53. Talts, J. F.; Weller, A.; Timpl, R.; Ekblom, M.; Ekblom, P. Regulation of mesenchymal extracellular matrix protein synthesis by transforming growth factor-beta and glucocorticoids in tumor stroma. J. Cell Sci. 108:2153–2162; 1995.
54. Tamkun, J. W.; Hynes, R. O. Plasma fibronectin is synthesized and secreted by hepatocytes. J. Biol. Chem. 258:4641–4647; 1983.
55. Wayner, E. A.; Garcia-Pardo, A.; Humphries, M. J.; McDonald, J. A.; Carter, W. G. Identification and characterization of the T lymphocyte adhesion receptor for an alternative cell attachment domain (CS-1) in plasma fibronectin. J. Cell Biol. 109:1321–1330; 1989.
56. Xia, P.; Culp. L. A. Adhesion activity in fibronectin's alternatively spliced EDa (EIIIA) and its neighboring type III repeats: Oncogene-dependent regulation. Exp. Cell Res. 213:253–265; 1994.